# Regulation of the RNA-binding protein Smaug by the GPCR Smoothened via the kinase Fused

Lucia Bruzzone[1,†], Camilla Argüelles[1,†], Matthieu Sanial[1,*,†] (ID), Samia Miled[1] (ID), Giorgia Alvisi[1], Marina Gonçalves-Antunes[1], Fairouz Qasrawi[1], Robert A Holmgren[2], Craig A Smibert[3,4], Howard D Lipshitz[4], Graciela L Boccaccio[5], Anne Plessis[1,‡,**] (ID) & Isabelle Bécam[1,‡,***] (ID)

## Abstract

From fly to mammals, the Smaug/Samd4 family of prion-like RNA-binding proteins control gene expression by destabilizing and/or repressing the translation of numerous target transcripts. However, the regulation of its activity remains poorly understood. We show that Smaug's protein levels and mRNA repressive activity are downregulated by Hedgehog signaling in tissue culture cells. These effects rely on the interaction of Smaug with the G-protein coupled receptor Smoothened, which promotes the phosphorylation of Smaug by recruiting the kinase Fused. The activation of Fused and its binding to Smaug are sufficient to suppress its ability to form cytosolic bodies and to antagonize its negative effects on endogenous targets. Importantly, we demonstrate *in vivo* that HH reduces the levels of *smaug* mRNA and increases the level of several mRNAs downregulated by Smaug. Finally, we show that Smaug acts as a positive regulator of Hedgehog signaling during wing morphogenesis. These data constitute the first evidence for a post-translational regulation of Smaug and reveal that the fate of several mRNAs bound to Smaug is modulated by a major signaling pathway.

## Introduction

A challenge in cell and developmental biology is to understand how inter- and intracellular signaling systems control gene expression. While post-transcriptional regulation of numerous cytoplasmic transcripts is known to play key roles in gene expression by modulating their stability, localization, and/or translation (see for review [1]), knowledge of how these processes are regulated by cell signaling remains rudimentary (see for instance, [2]). Cytoplasmic mRNA regulation is mediated by RNA-binding proteins (RBPs) and non-coding RNAs which co-recruit specific sets of mRNAs and protein factors that regulate mRNA fate [1]. Notably, these RBPs and their bound mRNAs often form dynamic membrane-less organelles (ribonucleoprotein (RNP) granules) with liquid droplet-like behavior and whose assembly can be dynamically regulated in response to external and internal factors [3–7].

Studies of oogenesis and early embryogenesis in *Drosophila melanogaster* have been instrumental in the identification of the biological functions of cytoplasmic RBPs as well as the underlying molecular mechanisms (see for instance [8–12]). The RBP Smaug plays key roles in fly early development as it is required for the correct anteroposterior polarization of the embryo and for the clearance of hundreds, if not thousands, of target mRNAs during the *Drosophila* maternal-to-zygotic transition [11,13–17]. Smaug is conserved throughout eukaryotes, and in mammals, there are two Smaug genes which control synapse biology, muscle growth, osteoblastogenesis, bone development, and the fate of embryonic neural precursor cells [18–22].

Smaug proteins bind their target transcripts via a conserved sterile alpha motif (SAM) domain that recognizes short stem/loop RNA structures [23,24] and recruit proteins that repress translation or/and induce transcript degradation [25–27]. Both in mammals and in insects, Smaug proteins form cytosolic bodies [25,28]. Notably,

Vts1, the yeast SMAUG protein has recently been shown to form self-templating condensates with prion-like behavior. Despite important sequence divergence, this characteristic has been conserved in evolution, as it is also observed for hSmaug1 [29].

While the multiplicity of Smaug's targets, mechanisms of action, and roles point to the importance of fine-tuning its spatio-temporal function, the molecular mechanisms that underlie its regulation are not well understood. Here, we reveal an unexpected connection between *Drosophila* Smaug and Smoothened, a G-protein Coupled Receptor (SMO) required for the transduction of the Hedgehog signal (HH) [30,31]. We demonstrate using fly cells that Smaug physically interacts with SMO and that SMO activation by HH leads to Smaug phosphorylation and its recruitment to the inner surface of the plasma membrane. Using a novel assay for Smaug-mediated repression, we show that HH/SMO signaling can both reduce Smaug protein levels and decrease its mRNA repressive activity. This latter effect relies on SMO promoting Smaug phosphorylation via the recruitment and activation of another positive regulator of HH signaling, the protein kinase Fused (FU) [32]. Forcing the association between an activated form of FU and Smaug promotes Smaug phosphorylation and recapitulates all the effects of HH/SMO on Smaug. Activated, Smaug-bound FU also suppresses the formation of cytosolic bodies of Smaug protein. Finally, using the wing imaginal disk as a model, we also demonstrate that HH downregulates the levels of *smaug* transcripts and upregulates endogenous mRNAs that had been identified to be bound and regulated by Smaug. We also show that *smaug* and *fu* mutants genetically interact. Together, these data constitute the first evidence that Smaug activity and ability to form cytoplasmic foci can be regulated by a signaling pathway via phosphorylation and reveal that Smaug could act as a positive modulator of HH signaling.

# Results

## Smaug interacts with SMO

We identified Smaug as a protein that binds to the cytoplasmic carboxy-terminal tail of *Drosophila* SMO (amino acids (aa) 558–1,036, hereafter referred to as the cytotail) through a two-hybrid screen. As activation of SMO involves the phosphorylation of the cytotail at a number of protein kinase A (PKA) sites, our screen employed a construct, "SMO$^{PKA-SD}$ cytotail" where all of modified serine (S) residues were mutated to aspartate (D), which mimics its activated state [33]. This screen led to the identification of 258 hits corresponding to 38 prey genes (see Appendix Table S1). Among the 5 preys that have the highest Predicted Biological Score (PBS) [34], FU was found as expected since it is a known partner of SMO [35]. Strikingly, Smaug was the most frequent prey and represented 137 of the positive hits.

We confirmed the interaction between SMO and Smaug by coimmunoprecipitation assays in *Drosophila* Cl8 cells, which are wing disk-derived cells known to respond to HH [36]. Full-length wild-type SMO or SMO$^{PKA-SD}$ tagged at their carboxy terminus with an HA epitope (SMO$^{WT}$-HA, SMO$^{PKA-SD}$-HA, respectively) and full-length, wild-type Smaug amino terminally tagged with a Myc epitope (Myc-Smaug$^{WT}$) were expressed either alone or together. Note that such

epitope tags were previously shown not to interfere with the normal functions of SMO and Smaug, respectively [27,35]. Protein complexes immunoprecipitated with an anti-HA antibody were analyzed by Western blot, which showed that Myc-Smaug$^{WT}$ coimmunoprecipitated with SMO$^{PKA-SD}$-HA as well as with SMO$^{WT}$-HA both in the presence and in the absence of HH (Fig 1A).

Our two-hybrid screen identified the region of Smaug between aa 74 and 291 as sufficient to bind SMO (Fig 1B). Consistent with this result, a region from aa 69 to 287 coimmunoprecipitated with SMO$^{WT}$-HA (Figs 1B and EV1A and B). This region includes two conserved domains known as Smaug similarity regions (SSR) 1 and 2. SSR1 functions as a dimerization domain [37] and, while the role of SSR2 is unknown, a missense mutation in this domain in one of the mouse Smaug proteins, SAMD4, results in a loss-of-function phenotype, suggesting that it plays an important role [19]. Deletion of either SSR1 or SSR2 blocks Smaug's interaction with SMO$^{WT}$-HA, suggesting that both are necessary for this interaction (Fig EV1B and C). Deletion analysis of the SMO cytotail showed that the carboxy-terminal 79 aa of SMO are both necessary and sufficient for its interaction with Smaug (Figs 1C–E and EV1D–F). Notably, this SMO region partially overlaps with a motif that binds the kinase FU, and is embedded in four clusters of S/T residues (green boxes in Fig 1C) whose phosphorylation is known to be induced by FU [38].

The activation of SMO by HH is associated with the phosphorylation of numerous sites in its intracellular C-terminal tail, which can easily be detected as it leads to slower electrophoretic mobility [39,40]. Examination of input (In) and immunoprecipitated (IP) fractions of SMO$^{WT}$-HA revealed that only unphosphorylated and/or partially phosphorylated SMO$^{WT}$-HA were associated with Myc-Smaug$^{WT}$ (Fig 1F, left panel). In contrast, the most hyperphosphorylated forms of SMO remained in the supernatant (Sup) after the immunoprecipitation. This hyperphosphorylation is known to involve the sequential action of multiple kinase including the protein kinase A (PKA), the casein kinase I (CKI), and FU [38,39]. However, the loss of Smaug interaction with hyperphosphorylated SMO does not involve the phosphorylation of the PKA, CKI, or FU phosphosites, as a mutant version of SMO where all of the PKA, CKI, and FU phosphosites are mutated to D residues is still converted to a hyperphosphorylated form that inefficiently coIPs with Smaug (Fig EV1G and I). Moreover, this hyperphosphorylated form and its reduced interaction with Smaug do not depend on a putative phosphorylation of the S and T residues present in the region of SMO that binds Smaug, as their mutation into A did not allow the hyperphosphorylated SMO to interact with Smaug (Fig EV1H and J).

In summary, these data show that Smaug and SMO cytotail can physically interact both in the absence and in the presence of HH. However, the highest level of SMO hyperphosphorylation is associated with a reduction in its interaction with Smaug.

## Activated SMO recruits Smaug to the plasma membrane

SMO activation is also associated with its relocalization from vesicles to the plasma membrane where it recruits an intracellular transducing complex that includes the protein kinase FU [39]. We therefore analyzed whether SMO could colocalize with Smaug and affect its localization, using SMO and Smaug fusions to fluorescent tags in transfected Cl8 cells (Fig 1G). As expected [40,41], SMO$^{WT}$-mCherry

(SMO$^{WT}$-mCh) was present in intracellular vesicles and was relocated to the plasma membrane in response to HH (Fig EV2A). As previously described in *Drosophila* and others organisms [28,29], GFP-Smaug$^{WT}$ was present in cytosolic bodies (hereafter referred to as S-bodies and that are likely self-templating condensates-HA), and we found that the presence of these bodies was unaffected by HH (Fig 1G1-2). When co-expressed in the absence of HH, SMO$^{WT}$-mCh and GFP-Smaug$^{WT}$ always (in 25/25 cells) strongly colocalized in cytosolic foci (Fig 1G3-3″). Strikingly, in the presence of HH, GFP-Smaug$^{WT}$ was, instead, concentrated at or near the cell surface where it colocalized with SMO$^{WT}$-mCh (Fig 1G4-4″). In all (45/45) of the cells showing SMO at the cell surface, Smaug was also localized at the periphery. This change in GFP-Smaug$^{WT}$ localization depends on its interaction with SMO, as it was not observed with SMO$^{\Delta958}$-mCh, which lacks its Smaug interaction region but is still localized to

the cell surface in the presence of HH (Fig EV2B). A similar relocalization of Smaug$^{WT}$ at the cell surface was also observed when co-expressed with SMO$^{PKA-SD}$ or SMO$^{PKA-SD\ FU-SD}$ (in which the PKA and FU phosphorylated Serines (S) and Threonines (T) sites are changed to aspartic acids (D) to mimic their phosphorylation), which both accumulate at the cell surface in the absence of HH (Fig EV2C). These results seem at odds with the observation that cell surface SMO is associated with its hyperphosphorylation [33], a state that seems to prevent its interaction with Smaug. To confirm that Smaug interacts with SMO at the plasma membrane, we specifically labeled the SMO molecules that are present at the cell surface using an extracellular N-terminal SMO fusion to the versatile SNAP tag that was labeled with a non-permeable fluorescent substrate in intact cells (Fig EV2D). Smaug also systematically colocalized with the SNAP-SMO$^{PKA-SD\ FU-SD}$ present at the cell surface (Fig EV2C). We then
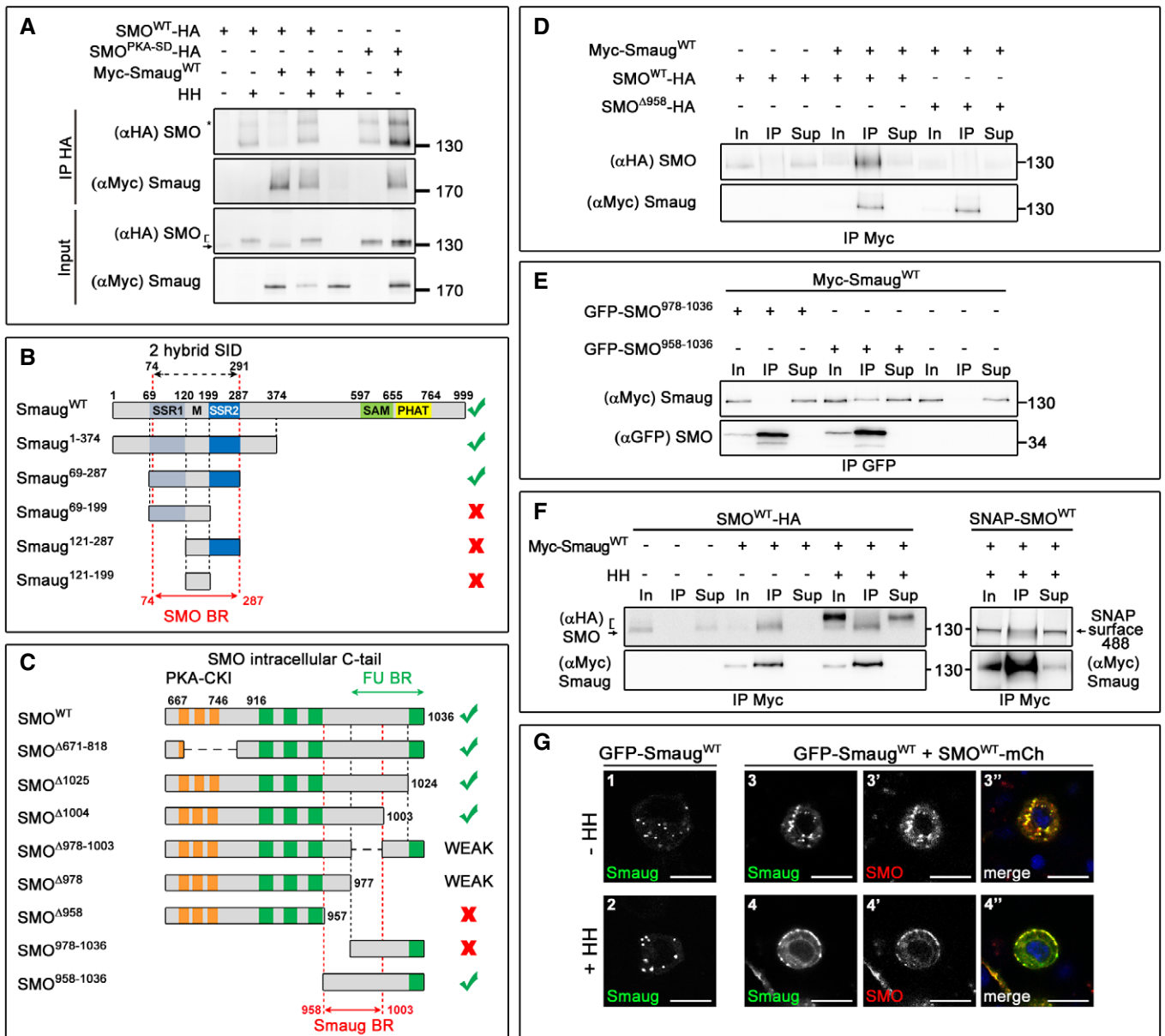


**Figure 1.**

**Figure 1. Smaug and SMO physically interact and colocalize.**

A  Coimmunoprecipitation of SMO-HA and Myc-Smaug proteins. Extracts of Cl8 cells expressing combinations of SMO$^{WT}$-HA or SMO$^{PKA-SD}$-HA with Myc-Smaug$^{WT}$ in the absence or presence of HH were immunoprecipitated (IP) with anti-HA. The input (lower panel) and the IP complexes (upper panel) were analyzed by Western blot with anti-Myc (αMyc) or anti-HA (αHA) antibodies. Here and in the other figures, the names of the proteins detected are indicated on the left and the molecular weights on the right, in kDa; the samples loaded for the input and the supernatants are equivalent to a tenth of the volume loaded for the IPs. * corresponds to higher molecular weight forms of SMO of unknown origin. Here and in panel F, the black arrow indicates unphosphorylated SMO$^{WT}$-HA and the bracket indicates the phosphorylated forms of SMO$^{WT}$-HA or SMO$^{PKA-SD}$-HA. All of the coIP data were independently reproduced at least twice.

B  Schematic representation of the domain structure of the Smaug protein. The conserved SSR 1 and 2 are shown in blue. They are separated by a 79 amino-acid-long non-conserved region (here referred to as "M"). The sterile alpha motif (SAM) domain is in green and the pseudo heat analogous topology domain (PHAT domain, which increases the affinity of the SAM domain for SRE) in yellow. The dashed double-arrow line at the top represents the smallest interacting region (called SID for smallest interacting domain) found according to the two-hybrid screen. The truncated constructs used are presented below. The ability to interact with SMO$^{WT}$-HA is indicated on the right: in green for yes, red for no. The full red double-arrow line below represents the smallest SMO-binding region (BR) that we could identify. The amino acid numbers correspond to Smaug-PA. (http://flybase.org/reports/FBgn0016070.html). See also Fig EV1A–C.

C  Schematic representation of the C-terminal "cytotail" of SMO. The PKA/CKI and FU phosphorylated regions are indicated as orange and green boxes, respectively. The FU-binding region (BR) is indicated by a full green double arrow above. The truncated constructs used are presented below, and their ability to coIP with Myc-Smaug$^{WT}$ is indicated on the right. The full red double-arrow line at the bottom represents the smallest Smaug-binding region (BR) identified in this work.

D, E  Mapping of the Smaug interaction domain in SMO. Extracts from Cl8 cells transfected with Myc-Smaug$^{WT}$ and various regions of SMO fused to either HA (D) or to GFP (E) were immunoprecipitated with αMyc (D) or αGFP (E) and analyzed by Western blotting with αMyc (lower panel in D and upper panel in E), αHA (D, upper panel), or αGFP (E, lower panel). In: Input; Sup: supernatant. See also Fig EV1D–F.

F  Hyperphosphorylated forms of SMO do not interact with Smaug. *Left panel:* Extracts of Cl8 cells expressing SMO$^{WT}$-HA with or without Myc-Smaug$^{WT}$ in the absence or presence of HH were IP with an αMyc antibody before analysis by Western blot with αHA (upper panel) or αMyc antibodies (lower panel). *Right panel:* Cl8 cells expressing SNAP-SMO$^{WT}$ with Myc-Smaug$^{WT}$ in the presence of HH were extracellularly labeled with a membrane-nonpermeable fluorescent SNAP substrate before cell lysis and immunoprecipitation (IP) with anti-Myc. Labeled SNAP-SMO was directly visualized after electrophoresis. Note its presence in the IP fraction with a relative enrichment of the less phosphorylated forms compared to the hyperphosphorylated forms. See also Fig EV1G–J.

G  SMO and Smaug colocalize. Representative fluorescent images of Cl8 cells expressing GFP-Smaug$^{WT}$ alone (1-2) or together with SMO$^{WT}$-mCherry (3–3″ and 4–4″) either without (1, 3–3″) or with HH (2, 4–4″). The merge images in 3″ and 4″ show GFP-Smaug$^{WT}$ in green and SMO$^{WT}$-mCh in red. The same results were seen with different fluorescent tags as well (Fig EV2B). The lack of effect of HH on GFP-Smaug$^{WT}$ in the absence of SMO$^{WT}$-mCh is likely due to limiting amounts of endogeneous SMO. At least 20 cells were assayed for each condition. In the absence of HH, all co-transfected cells exhibited greater than 90% colabeled SMO$^{WT}$-mCherry. Scale bar (shown in G1, identical for all panels): 10 μm. See also Fig EV2.

coexpressed Myc-Smaug with SNAP-SMO$^{WT}$ in the presence of HH, and we labeled specifically the SNAP-SMO$^{WT}$ molecules present at the cell surface before cell lysis and immunoprecipitation of Myc-Smaug. Direct analysis after electrophoresis of the coimmunoprecipitated fraction revealed that SNAP-SMO$^{WT}$ present at the cell surface interacted with Myc-Smaug (Fig 1F, right panel).

Together, these data show that SMO and Smaug physically interact and colocalize in cytoplasmic foci and that in response to HH signaling, a fraction of activated SMO that is present at the cell membrane directly recruits Smaug.

### Activated SMO attenuates Smaug repressive effects and levels

The observed interaction between Smaug and SMO and the relocalization of Smaug to the plasma membrane by SMO suggest that HH/SMO might affect Smaug's ability to repress target mRNA expression. As SMO did not bind Smaug at or near the SAM domain, we speculated that it would regulate the repressive activity of Smaug rather than its ability to bind target mRNAs and chose to develop a tethering assay that allowed us to simultaneously monitor both Smaug levels and repression capacity in Cl8 cells (Fig 2A). This assay is an adaptation of dual tethering assays that exploit a peptide derived from the bacteriophage lambda λ N protein, which binds with high specificity and affinity to an RNA stem-loop structure known as BoxB [42–44]. Smaug was fused to the λN peptide, and a glucuronidase (GUS, *from A. thaliana*) reporter mRNA was generated carrying five BoxB stem-loops in its 3′-untranslated region (3′UTR). Both λN-Smaug and GUS proteins were also fused to the SNAP self-labeling peptide (leading to λN-SNAP-Smaug and SNAP-GUS, respectively) allowing their respective levels to be simultaneously and directly quantified after fluorescent tagging and

electrophoresis [45]. An irrelevant construct encoding a SNAP-GFP fusion served as an internal control for transfection and protein recovery efficiencies.

First, we validated our system by verifying that λN-SNAP-Smaug repressed SNAP-GUS levels 2- to 2.5-fold in a manner that depended upon both the BoxB sites in the reporter mRNA and the expression of λN-SNAP-Smaug (Figs 2B and C, and EV3A and B). Given the nature of our assay, the decrease in the SNAP-GUS reporter levels could reflect a reduction in the levels of the *snap-gus-5BoxB* mRNA, of its translation or both. We therefore monitored the amount of *snap-gus-5BoxB*-GUS mRNA by reverse transcription followed by quantitative PCR (RT–qPCR). As shown in Fig EV3C, λN-SNAP-Smaug reduces the amount of *snap-gus-5BoxB*-GUS mRNA almost twofold. Although we cannot exclude additional translational regulation, this indicates that λN-SNAP-Smaug reduces stability of the reporter mRNA.

Next, we assayed the effect of HH/SMO on the expression of the reporter in the presence of λN-SNAP-Smaug (Figs 2D and EV3D). While SMO$^{WT}$-HA or HH alone had no statistically significant effect, SMO$^{WT}$-HA in the presence of HH led to an increase in SNAP-GUS levels indicating a reduction in λN-SNAP-Smaug-dependent repression. A similar effect was seen with SMO$^{PKA-SD}$-HA in the absence of HH. The effects of SMO$^{WT}$-HA or SMO$^{PKA-SD}$-HA on the reporter reflected a reduction in its repression by λN-SNAP-Smaug rather than a direct, Smaug-independent, effect as they had no significant effect on the reporter in the absence of λN-SNAP-Smaug (Fig EV3E). Moreover, SMO$^{Δ958}$-HA which is unable to bind and colocalize with Smaug (see above) had no effect (despite the presence of HH; Figs 2D and EV3D). This strongly suggests that SMO needs to be associated with Smaug to negatively regulate the Smaug-bound reporter.
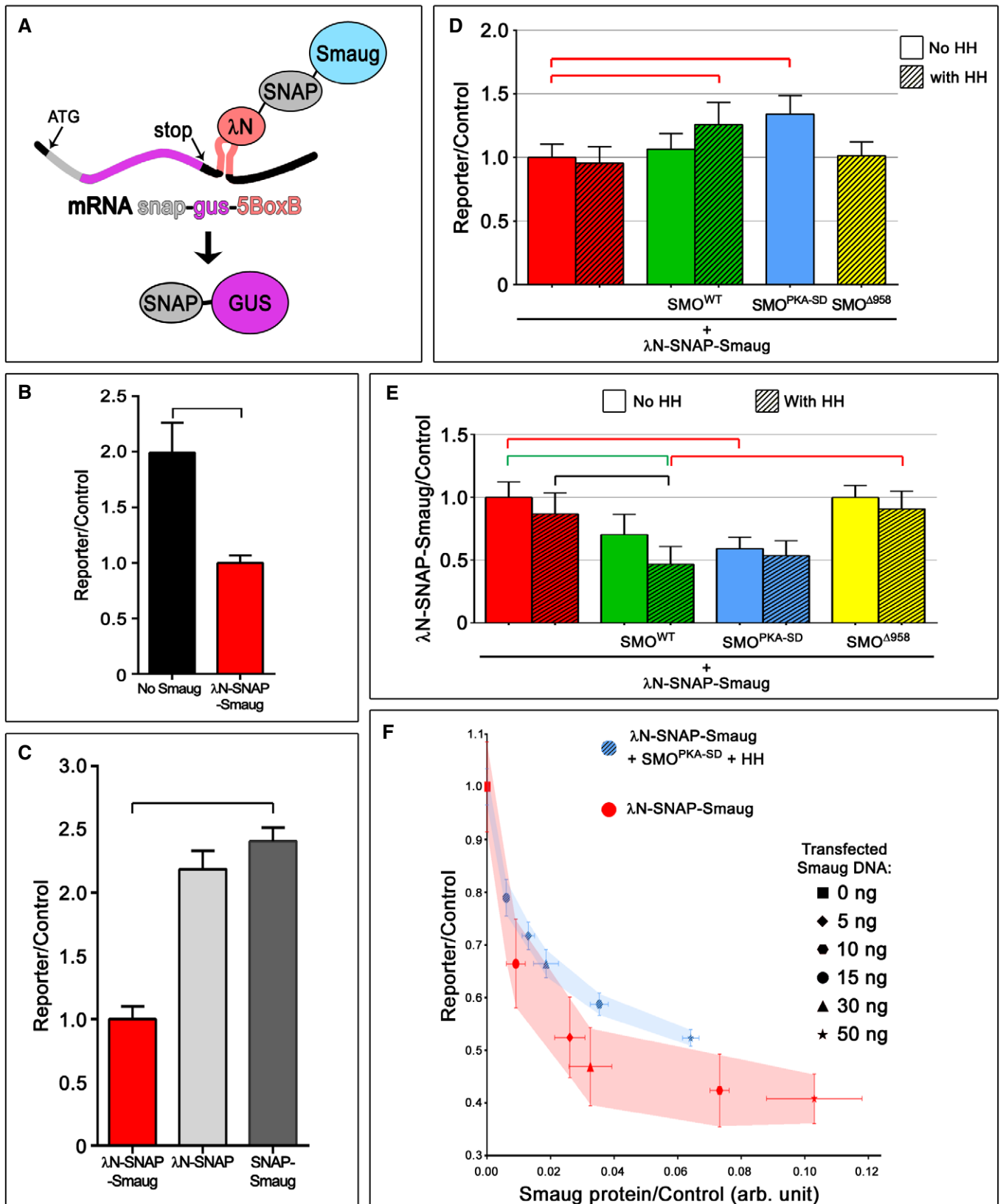
**Figure 2.**

**Figure 2. SMO/HH regulates Smaug levels and activity.**

A   Smaug repression assay. The assay is based on the dual expression of a construct encoding a λN-HA-SNAP-Smaug chimeric protein (abbreviated λN-SNAP-Smaug) and a second that is transcribed into a reporter mRNA (called *SNAP-GUS-5BoxB*) that carries a translational fusion between SNAP and GUS coding regions followed by five Box B hairpins (5BoxB) inserted in the 3'UTR. A plasmid encoding a GFP-SNAP fusion (not shown here) was also used as a transfection and loading control.

B, C   Smaug downregulates reporter expression. Mean values of the relative levels of SNAP-GUS reporter (SNAP-GUS/GFP-SNAP ratio, in arbitrary units) in extracts of transfected Cl8 cells in the absence (black) or presence of λN-SNAP-Smaug (red), λN-SNAP (pale grey), or SNAP-Smaug (dark grey). See Fig EV3A for the representative gel and Fig EV3B which shows that λN-SNAP-Smaug has no effect on a *SNAP-GUS* construct that lacks the 5BoxB. *N* = 3 (biological replicates). See also Fig EV3A–C. Here and in (D–F): SNAP-GUS/GFP-SNAP ratios were set to 1 in cells expressing λN-SNAP-Smaug. The error bars correspond to the standard deviation of the mean (SD). Statistical analysis was done by a Kruskal–Wallis test by ranks followed by a Dunn test, and *P* values are as follows: black bracket < 0.05, red bracket < 0.01, and green bracket < 0.0001. Here and in D–E: 15 ng of *pAct.λN-SNAP-smaug* plasmid was used per transfection.

D, E   HH/SMO reduces Smaug levels and its overall negative effect on reporter expression. Mean values of the relative levels of reporter expression (determined as above) (D) or of λN-SNAP-Smaug (ratio λN-SNAP-Smaug/GFP-SNAP) (E) in the absence of SMO constructs (red) or in the presence of SMO[WT]-HA (green), SMO[PKA-SD]-HA (blue) or SMO[Δ958]-HA (yellow), without HH (plain boxes) or in presence of HH (striped boxes). *N* = 6 (independent biological replicates), except for "no SMO, no HH" and "SMO[WT] with HH" conditions where *n* = 10 (independent biological replicates). A representative gel is shown in Fig EV3D. Note that SMO[WT]-HA or HH alone had reproducible weak effects that were observed in two independent biological triplicates but were not statistically significant. See also Fig EV3E and F.

F   HH/SMO reduces Smaug's intrinsic repressive ability. A similar experiment was conducted with different amounts of *λN-SNAP-smaug* expressing plasmid (ranging from 0 to 50 ng) as indicated. The mean values of the relative levels of reporter (*y*-axis) are plotted against the relative levels of λN-SNAP-Smaug (*x*-axis). SNAP-GUS/GFP-SNAP ratios were set to 1 in cells expressing λN-SNAP-Smaug in the absence of SMO[PKA-SD]/HH. The colored area represents the extent of the values observed for the relative amounts of reporter expression obtained with (blue) and without (red) SMO[PKA-SD]/HH, respectively. *N* = 3 (biological triplicates). See Fig EV3H and also a representative gel in Fig EV3G.

The upregulation of the SNAP-GUS reporter levels in the presence of activated SMO could be due, at least in part, to the downregulation of λN-SNAP-Smaug levels. We found that SMO[WT]-HA co-expression or the presence of HH alone had no statistically significant effect on λN-SNAP-Smaug levels (Figs 2E and EV3D). However, SMO[WT]-HA and HH together led to a significant decrease in Smaug levels. SMO[PKA-SD]-HA alone had a similar negative effect on λN-SNAP-Smaug levels which were not significantly increased by HH. Again, no effect was seen with SMO[Δ958]-HA (despite the presence of HH). The effect of SMO[PKA-SD]-HA on λN-SNAP-Smaug levels was associated with a similar reduction in the levels of its mRNA that was monitored by RT–qPCR (Fig EV3F).

Finally, to assess the contribution of the reduction in λN-SNAP-Smaug levels to the decrease in λN-SNAP-Smaug repressive activity, we monitored the expression of the SNAP-GUS reporter in response to different doses of λN-SNAP-Smaug, either in the absence or in the presence of SMO[PKA-SD]-HA (with HH) (Figs 2F and EV3G and H). We transfected the cells with different amounts of the *λN-snap-smaug* expression vector (ranging from 5 to 50 ng). As expected from the above results, the amounts of λN-SNAP-Smaug for a given dose of vector were always lower in the presence of SMO[PKA-SD]-HA/HH than in its absence. In both cases, the expression of the SNAP-GUS reporter decreased exponentially in a λN-SNAP-Smaug dose-dependent manner. However, for the same amount of λN-SNAP-Smaug protein, the levels of the SNAP-GUS reporter were systematically higher in the presence of SMO[PKA-SD]-HA and HH than in their absence, indicating that SMO activation reduces the intrinsic repressive activity of Smaug.

In summary these results reveal that SMO and HH signaling attenuate Smaug function in two ways: by reducing its levels and by downregulating its repressive activity. Both components depend on SMO activation and its ability to interact directly with Smaug.

**Figure 3. SMO/HH activation promotes the phosphorylation of Smaug.**

A   HH/SMO promotes slow-migrating forms of Smaug. Western blot analysis of Cl8 cells that transiently express HA-Smaug[WT] alone, or together with either SMO[WT]-GFP or SMO[PKA-SD]-GFP, in the presence or in the absence of HH. GMAP serves as a loading control. Here and in the other panels, the antibodies used are indicated on the left. Here and in (B, C), the black arrows indicate the unphosphorylated form of HA-Smaug[WT] and the brackets indicate the slower migrating phosphorylated forms of HA-Smaug[WT]. NT: not transfected. See a phosphatase assay in Fig EV4A.

B   Smaug phosphorylation requires its interaction with SMO. Western blot analysis of Cl8 cells expressing HA-Smaug[WT], in the presence of HH, in combination with SMO[Δ958]-GFP, SMO[PKA-SD]-GFP, or SMO[PKA-SD, Δ978]-GFP, as indicated.

C   FU controls Smaug phosphorylation. Extracts of Cl8 cells expressing SNAP-Smaug with SMO[PKA-SD FU-SD]-GFP (with HH) in combination with GFP-FU[WT], GAP-GFP-FU[WT], Myc-FU[EE], or GAP-GFP-FU[DANA] (as indicated) were labeled for the SNAP tag before electrophoresis. After quantification of the gels, the percentage (%) of phosphorylated Smaug (% of phosphorylated forms of SNAP-Smaug total amounts of SNAP-Smaug) was estimated. In (C–E), the mean values and SD for independent biological triplicates (*N* = 3) are shown in the graph at the bottom, and the statistical analysis was done by one-tailed bivariate Wilcoxon rank test. See also Fig EV4C and D.

D   Phosphorylation of Smaug by activated FU requires the co-expression of SMO. Mean values of the percentage of phosphorylated Smaug in extracts of Cl8 cells that express λN-SNAP-Smaug with GAP-GFP-FU[WT] and SMO[WT] alone or together (as indicated) *N* = 3 (biological triplicates). Note that the effect of GAP-GFP-FU[WT] and SMO[WT] together is lower than the one observed with GAP-GFP-FU[WT] and SMO[PKA-SD FU-SD]-GFP together (in panel C). This could have multiple nonexclusive causes, including the fact that SMO[WT] is present at much lower levels than SMO[PKA-SD FU-SD] [38] and/or the involvement of another kinase. See also Fig EV4B. Note that Smaug does not coIP FU unless SMO is present see Appendix Fig S2.

E   Forcing the interaction of Smaug with activated FU leads to a SMO-independent phosphorylation of Smaug. Mean values of the percentage of phosphorylated Smaug in Cl8 cells coexpressing λN-SNAP-Smaug with GFP-FU, FU-SBR, FU[EE]-SBR, or FU[DANA]-SBR, with or without HH, as indicated. *N* = 3 (biological triplicates). See also Fig EV4C and D. Note that the levels of Smaug phosphorylation observed in the presence of FU[DANA]-SBR are not lower than those seen with GFP-FU. This suggests an incomplete inhibition of endogenous FU, which may be due to the trapping of FU[DANA]-SBR by Smaug. See a representative blot in Fig EV3C and a phosphatase assay in Fig EV4D. The mapping of the phosphosites is shown in Fig EV4E–G.
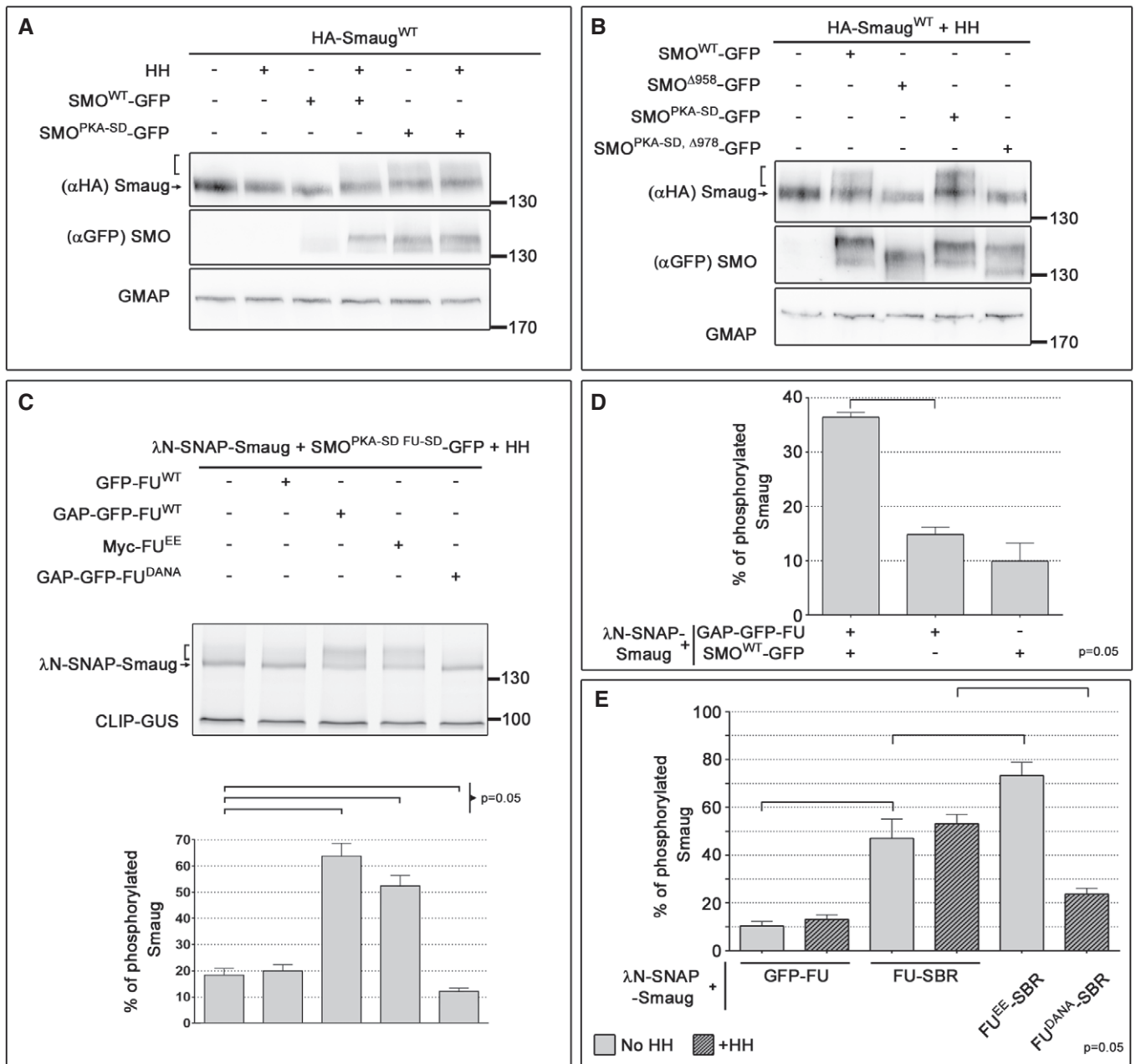
Figure 3.

## SMO activation promotes Smaug phosphorylation in a FU kinase-dependent manner

As HH signaling leads to the phosphorylation of many members of its pathway, we next tested the possibility that the effects of activated SMO on Smaug could be due to the phosphorylation of the latter. As shown in Fig 3A, SMO[WT]-GFP induced an electrophoretic mobility shift of HA-Smaug[WT] in the presence of HH, and this effect was absent either when SMO[WT]-GFP was not co-expressed or in the absence of HH. A similar shift was seen when HA-Smaug[WT] was co-expressed with SMO[PKA-SD]-GFP. In all cases, treatment of the extracts with a phosphatase [33,46,47] abolished the slower migrating forms induced by activated SMO, demonstrating that these are

phosphorylated forms of Smaug (Fig EV4A). These effects depended on the ability of SMO[WT]-GFP (and SMO[PKA-SD]-GFP) to interact with Smaug as SMO[PKA-SD, Δ978]-GFP and SMO[Δ958]-GFP were unable to induce the phosphorylation of HA-Smaug[WT] (Fig 3B). This is unlikely to be due to a lack of function of these SMO constructs since SMO[Δ978]-GFP is known to be constitutively active [35].

The kinase FU binds to the cytotail of SMO near the Smaug-binding region (see Fig 1C). In response to HH, SMO was shown to recruit FU to the plasma membrane promoting its activation and the phosphorylation of its targets including SMO itself and downstream members of the HH pathway [38,48,49]. This raised the possibility that FU could also be involved in the phosphorylation of Smaug upon HH/SMO activation. We therefore analyzed the effects of

different forms of FU in the presence of HH and SMO$^{PKA-SD\ FU-SD}$-GFP (Fig 3C): (i) GFP-FU$^{WT}$ [35]; (ii) GAP-GFP-FU$^{WT}$, which is constitutively activated through fusion of FU to the GAP43 palmitoylated domain, which targets the protein to the plasma membrane [32,50]; (iii) Myc-FU$^{EE}$, another activated form of FU, where Thr-151 and Ser-154 were both mutated to glutamate [51]; and (iv) GAP-GFP-FU$^{DANA}$ a kinase-dead form of GAP-FU. FU$^{DANA}$ overexpression is a common tool to downregulate endogenous FU activity as it acts in a dominant-negative fashion, likely via dimerization with endogenous FU [32,50]. We used SMO$^{PKA-SD\ FU-SD}$ (fused to GFP, SMO$^{PKA-SD\ FU-SD}$-GFP) in these experiments to avoid the effects of a known positive feedback between FU and SMO that occurs via the phosphorylation by FU of SMO's cytotail [38]. To ensure precise quantification, Smaug was fused to the SNAP peptide. In the presence of SMO$^{PKA-SD\ FU-SD}$-GFP alone, ~18% of SNAP-Smaug was phosphorylated. Co-expression of GFP-FU$^{WT}$ had no significant effect, whereas co-expression of the constitutively activated forms GAP-GFP-FU$^{WT}$ or Myc-FU$^{EE}$ further increased SNAP-Smaug phosphorylation by approximately 3- and 2.5-fold, respectively. In contrast, when GAP-GFU$^{DANA}$ was co-expressed, there was a 40% reduction in phosphorylated SNAP-Smaug (to ~12%) compared to SMO$^{PKA-SD\ FU-SD}$-GFP alone. This shows (i) that the induction of Smaug phosphorylation by GAP-GFP-FU depends on its kinase activity and (ii) that FU activation is, at least in part, required for the full induction of Smaug phosphorylation by activated SMO.

The above data indicate that SMO promotes Smaug phosphorylation by activating FU. The ability of SMO to bind both FU and Smaug through adjacent protein regions could bring them in close proximity, thereby facilitating phosphorylation of Smaug by FU. We, therefore, tested whether a constitutively active form of FU could promote the phosphorylation of Smaug in the absence of SMO co-expression. As shown in Fig 3D (and Fig EV4B), in the absence of HH, the percentage of phosphorylated SNAP-Smaug was more than twice as high when GAP-GFP-FU and SMO-GFP$^{WT}$ were expressed together than separately. This synergic effect indicates that SMO is required for the effects of activated FU, and we then tested whether co-expression of SMO was still necessary when we forced a direct interaction between FU and Smaug by fusing the Smaug-binding region (SBR) present in SMO to the N-terminus of wild-type or mutant forms of FU (Figs 3E and EV4C). Surprisingly, FU-SBR alone resulted in ~4× fold increase in SNAP-Smaug phosphorylation when compared to the levels observed in the presence of GFP-FU. A potential explanation for this activation of FU in the absence of HH is that a multimerization of Smaug may facilitate FU dimerization, an event known to be sufficient to promote its activation [52]. The phosphorylation of SNAP-Smaug was even higher with FU$^{EE}$-SBR (with more of 70% of Smaug being phosphorylated), while it was strongly reduced in the presence of FU$^{DANA}$-SBR (23% of phosphorylated Smaug), confirming the requirement for FU kinase activity.

Smaug contains 181 S and T (of a total of 999 amino acids). To map Smaug's phosphosites, we analyzed the effects of HH/SMO/FU on variants of *smaug* in which eleven large segments were, respectively, substituted by synthetic fragments in which the S/T codons were replaced by A codons (Fig EV4E–G). Two of the Smaug variants (Smaug$^{274-399\ SA}$ in which the 38 S/T of the region 5 that spans aa 274–399 were mutated and Smaug$^{400-502\ SA}$ in which the 15 S/T of the region 6 spanning aa 400–502 were mutated) showed a strong

reduction—but not a total suppression—in the phosphorylation shift induced by FU$^{EE}$-SBR or SMO/HH (Fig EV4F). Mutation of the 14 S/T is presented in the region between aa 372 and aa 434 a similar effect. This region contains three sequences (at positions 372, 394, and 434) that could correspond to a phosphorylation consensus site for FU $(S(X)_5D/E)$ [53]. Their simultaneous mutation led to a modest reduction in the percentage of Smaug molecules phosphorylated in the presence of FU$^{EE}$-SBR.

Together these data show that the FU kinase promotes—likely directly although we cannot exclude an indirect effect via another kinase that would remain to be identified—the phosphorylation of Smaug in response to HH/SMO signaling. This phosphorylation requires S/T-enriched regions located in the central region of Smaug, between the SSR1 and the SAM domain. In this process, it is likely that SMO both promotes FU activation and bridges it to Smaug.

### The FU kinase downregulates Smaug repressive activity

The induction of Smaug phosphorylation by HH/SMO signaling relies, at least in part, on the recruitment and activation of FU. This raised the possibility that FU could also mediate the negative effects exerted by HH/SMO signaling on Smaug. To test this, we further analyzed the effects of FU$^{EE}$-SBR on Smaug levels and repressive capacity. As shown in Figs 4A and EV5A, increasing levels of the *fu$^{EE}$-SBR* expression plasmid upregulated the percentage of λN-SNAP-Smaug phosphoforms in a dose-dependent manner, starting from a background of ~5% in the absence of *fu$^{EE}$-SBR* plasmid to almost 70% with 60 ng. In parallel, *fu$^{EE}$-SBR* expression upregulated the levels of SNAP-GUS reporter expression (Fig EV5A and B). This effect required the presence of λN-SNAP-Smaug (Fig EV5C). The expression of the reporter correlated with the fraction of phosphorylated λN-SNAP-Smaug (Fig 4B). This indicates that the phosphorylation of λN-SNAP-Smaug induced by activated FU could reduce its repressive activity on the SNAP-GUS reporter. In addition, *fu$^{EE}$-SBR* expression also downregulated λN-SNAP-Smaug protein levels (Figs 4C and EV5A). This latter effect did not vary with the dose of *fu$^{EE}$-SBR* and did not depend on the percentage of phospho-Smaug induced by *fu$^{EE}$-SBR*. Moreover, the kinase-inactive form, FU$^{DANA}$-SBR, also downregulated Smaug levels (Fig EV4D and E), which indicates that FU regulates Smaug levels independently of its kinase activity.

In conclusion, these data show that the FU kinase induces the phosphorylation of Smaug and negatively regulates Smaug by at least two means: It attenuates Smaug's mRNA repressive activity in a phosphorylation-dependent manner and reduces Smaug levels independent of its kinase activity.

### The FU kinase suppresses S-body formation

We next addressed whether FU$^{EE}$-SBR has an effect on Smaug's subcellular distribution (Fig 4D). We co-expressed GFP-Smaug$^{WT}$ with FU$^{EE}$-SBR tagged with mCherry. Strikingly, the presence of FU$^{EE}$-SBR-mCh completely suppressed the formation of GFP-Smaug$^{WT}$ bodies, leading to a more uniform distribution. The effect was due to the kinase activity of FU$^{EE}$-SBR-mCh, as the kinase-dead form of FU did not affect S-body formation. Whereas FU$^{EE}$-SBR-mCh alone displayed diffuse cytoplasmic localization both in the presence
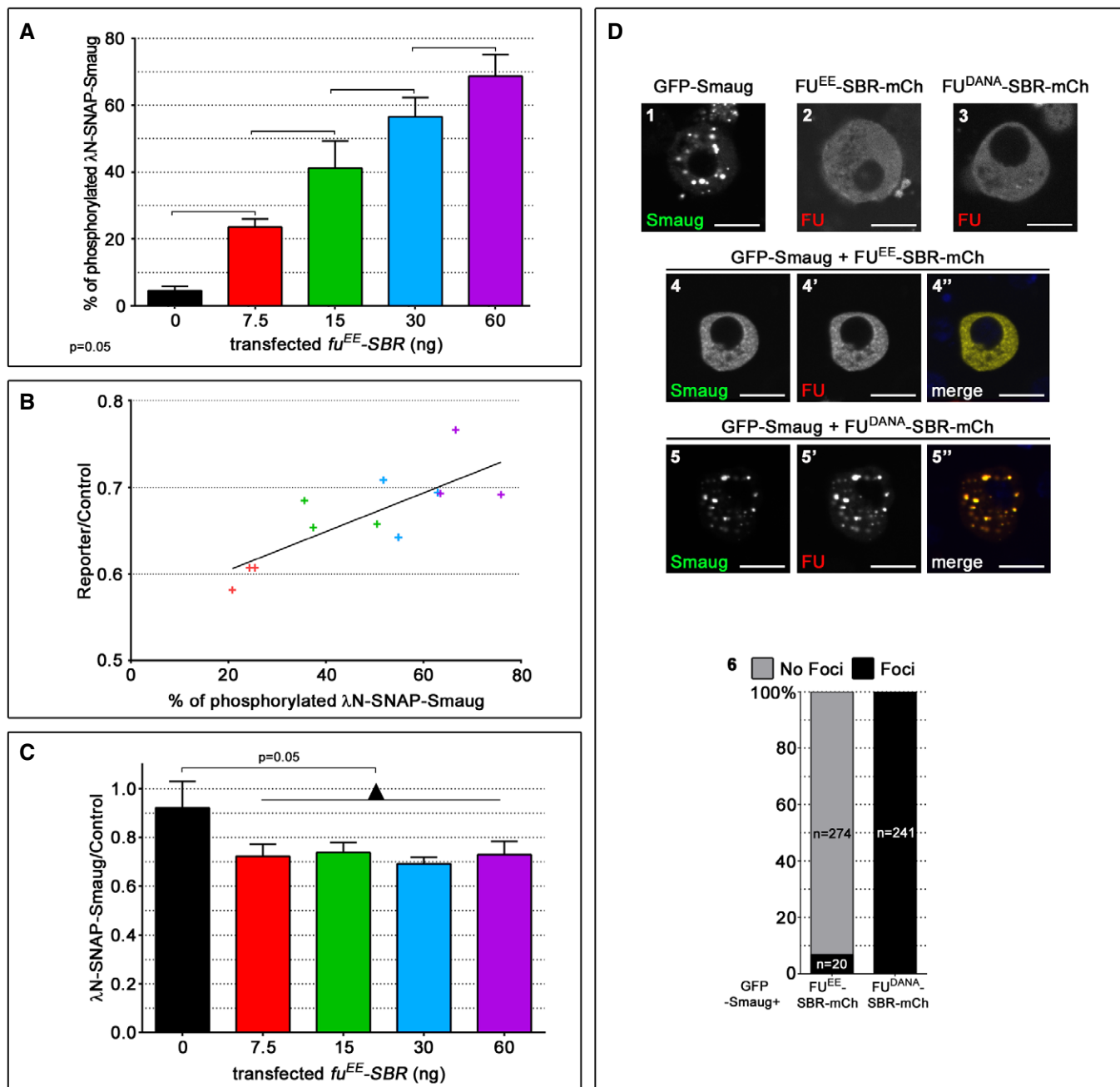
**Figure 4. FU downregulates Smaug levels and repressive effect.**

A, C  Effect of FU$^{EE}$-SBR on Smaug phosphorylation and levels. Extracts of Cl8 cells transfected with *λN-SNAP-smaug* (25 ng) and *SNAP-GUS-5BoxB* (300 ng) plasmids in the absence or with different amounts of FU$^{EE}$ expressing plasmid (ranging from 15 to 60 μg, as indicated) were analyzed by electrophoresis before quantification as above. See a representative gel in Fig EV5A. The % of phosphorylated SNAP-Smaug protein (determined as in Fig 3) (A) and relative levels of λN-SNAP-Smaug protein (C) (determined as in Fig 2) are represented as a function of the levels of FU$^{EE}$-SBR. The mean values and SD for independent biological triplicates (*N* = 3) are shown in the graph at the bottom. The statistical analysis was done by one-tailed bivariate Wilcoxon rank test with a *P* value = 0.05 (*). Here, CLIP-GUS was used as an internal control.

B  Effect of FU$^{EE}$-SBR on Smaug activity. The relative levels of reporter expression obtained in the same experiment as in (A, C) are represented as a function of the % of phosphorylated Smaug. Color of data points corresponds to ng of transfected FU$^{EE}$-SBR in (A–C). See also Fig EV5B–D.

D  Effect of FU$^{EE}$-SBR on Smaug subcellular localization. Representative fluorescent images of Cl8 cells expressing GFP-Smaug$^{WT}$ (1), FU$^{EE}$-SBR-mCherry (2), FU$^{DANA}$-SBR-mCh, (3) or expressing GFP-Smaug$^{WT}$ together with FU$^{EE}$-SBR-mCherry (4–4″) or GFP-Smaug$^{WT}$ together with FU$^{DANA}$-SBR-mCh (5–5″). The merge images in 4″ and 5″ show GFP-Smaug$^{WT}$ in green and FU$^{EE}$-SBR-mCh or FU$^{DANA}$-SBR-mCh in red. (6) In the presence of FU$^{EE}$-SBR, 274 of a total of 294 cotransfected cells show a diffuse localization of Smaug and FU and no foci. In the presence of FU$^{DANA}$-SBR, 100% of the cotransfected cells (*n* = 241) show Smaug and FU distributed in bodies and colocalized. 250 ng of plasmid was used for each construct. Scale bar (shown in D1, identical for all panels): 10 μm.

or in the absence of GFP-Smaug, the kinase-dead FU$^{DANA}$-SBR-mCh was mostly found to colocalize with the S-bodies. Note that the drop in Smaug levels described above is not the cause of the absence of S-bodies in the presence of FU$^{EE}$-SBR-mCh as both FU constructs have a similar effect on Smaug levels.

### The FU kinase upregulates Smaug endogenous targets

We next examined whether HH/SMO/FU could also regulate endogenous Smaug target mRNAs in Cl8 cells. We assessed the effect of FU$^{EE}$-SBR on the endogenous levels of thirteen Smaug mRNA targets that include the following: (i) its well-characterized mRNA target *Hsp83*, (ii) five mRNAs that were among the top 15 Smaug targets from early embryo data (as defined by their enrichment in Smaug IPs and the extent of stabilization and translational upregulation in *smaug* mutants compared to wild type; Chen *et al* [13] and Tadros *et al* [15], and (iii) eight mRNAs that were shown to bind Smaug and encode mitochondrial proteins [54]. These latter mRNA were chosen as HH signaling was reported to regulate mitochondrial function. FU$^{EE}$-SBR significantly upregulated the levels of eighth of these mRNAs (Figs 5A and EV5E). These effects require the kinase activity of FU and its binding to Smaug (to a lesser extend) as FU$^{DANA}$-SBR and FU$^{EE}$ had no or little effect, respectively. Importantly, in almost all cases that we tested *SMO*$^{PKA-SD}$ (with HH) recapitulated the effects of FU$^{EE}$-SB*R*: It increases the levels of *ND-23*, *ND-75*, *Rpn1*, and *RFeSP* that were affected by FU$^{EE}$-SBR but had no significant effect on *ND-42* and *SdhA* transcripts that were also not significantly affected by FU$^{EE}$-SBR.

Next, we tested whether HH signaling affected the function of Smaug *in vivo* using as a model the wing imaginal disk, whose development is controlled by HH. We tested the effects of HH on five of the mRNAs that were regulated by FU$^{EE}$-SBR and/or HH/SMO$^{PKA-SD}$ in the Cl8 cells *(Gapdh2, COX7, ND-23, ND-75,* and *Rpn1)*. As shown in Fig 5B, overexpression of hh in the whole wing pouch (using the UAS/GAL4 system) strongly (from twofold to ninefold, depending on the mRNAs) increased the levels of *all these* transcripts (compared to a control that expresses a GFP under the GAL4 driver) and conversely, the inactivation of HH activity using a thermosensitive allele (*hh*$^{ts2}$) at restrictive temperature significantly downregulated their level when compared to a wild-type strain raised at the same temperature). Notably, these effects revealed opposing responses of *smaug* mRNA levels to manipulations of HH as they are upregulated when HH levels are increased and reduced (from x to y folds) when HH is inactivated.

In summary, our *in vivo* data demonstrate that in both transfected Cl8 cells and fly, HH/SMO signaling decreases the levels of the *smaug* mRNA and downregulates the levels of several of its mRNA targets.

### *smaug* and *fu* genetically interact during wing morphogenesis

Taken together our results suggest that Smaug may be involved in the regulation of HH signaling. *smaug* loss-of-function mutants are viable and display no obvious adult phenotypes [55]. However, since the effects of loss of another FU-binding partner and target, SU (FU), are only visible in the absence of FU kinase activity [56], we tested the effect of the *smaug*$^{47}$ mutation in combination with *fu*$^1$, an allele that encodes a kinase-dead form of FU [56]. *fu*$^1$ leads to a mild defect in wing patterning characterized by a narrowing of the intervein between longitudinal veins 3 and 4 (LV3-4). As this *fu*$^1$ phenotype is somewhat variable, we categorized it as "weak" when the fusion of LV3-4 was mainly visible in the proximal region (with only a limited distal fusion near the wing margin) and as "strong" when the fusion was more extensive and/or when anastomoses were present between the two LVs (Appendix Fig S4). As shown in Fig 5C, *fu*$^1$/Y; *smaug*$^{47}$/*smaug*$^{47}$ double-mutant males displayed a strong LV3-4 fusion phenotype more than twice as often as the *fu*$^1$/Y or *fu*$^1$/Y; *smaug*$^{47}$/+ control males. This indicates that a *smaug* loss-of-function mutation genetically enhances the effect of the *loss of activity of the FU kinase*, suggesting that Smaug can positively contributes to HH signaling to pattern the wing.

## Discussion

This work uncovers an unexpected interplay between HH/SMO signaling and the RBP Smaug in *Drosophila*. In brief, using wing-cultured cells Cl8 cells as a "test tube", we identified and reconstituted a "HH/SMO/FU pathway" that regulates Smaug. We show that it promotes its phosphorylation, downregulates its levels, and reduces its repressive activity. All these effects rely on the GPCR SMO acting as a scaffold bridging Smaug with the protein kinase FU which promotes Smaug's phosphorylation. Forcing the interaction between Smaug and activated FU recapitulates the effects of HH/SMO on Smaug. Moreover, it reduces the endogenous levels of its target mRNAs and inhibits the formation of the cytoplasmic S-bodies. Importantly, HH/SMO/FU also regulates the endogenous targets of Smaug both in cultured cells and in *in vivo*. Finally, *smaug* and *fu* genetically interact to modulate wing patterning, revealing a so far unsuspected role of Smaug in *Drosophila* development as a positive modulator of HH signaling.

Based on these data, we propose that HH regulates via SMO and FU the fate of mRNAs bound to Smaug, leading to positive modulation of HH signaling. These data support the following model (presented in Fig 6). In the absence of HH, Smaug forms S-bodies and promotes the decay of its target mRNAs. It also binds SMO which is present on intracellular trafficking vesicles. In response to HH, SMO activates FU and this promotes the phosphorylation of Smaug leading to the disappearance of the S-bodies and release of the bound mRNAs, leading to their accumulation. Similarly, a transient dissolution of the Smaug/SAMD4 bodies was reported in the post-synaptic region of rat neurons upon stimulation of specific receptors [18,57–59].

### A novel reporter to monitoring Smaug repressive effects

We developed a novel Smaug repression assay that allows—thanks to the SNAP tag—the simultaneously evaluation of Smaug repressive activity and levels. This permits the evaluation of variations in Smaug levels on the global changes in reporter expression. This reporter also allows the specific monitoring of changes in Smaug's ability to repress mRNAs, independently of its ability to bind them. Smaug has been shown to act on its target mRNAs either through an inhibition of their translation or by promoting their degradation after deadenylation, depending on the proteins that it recruits [11,27,60]. Here, Smaug has comparable effects on the protein
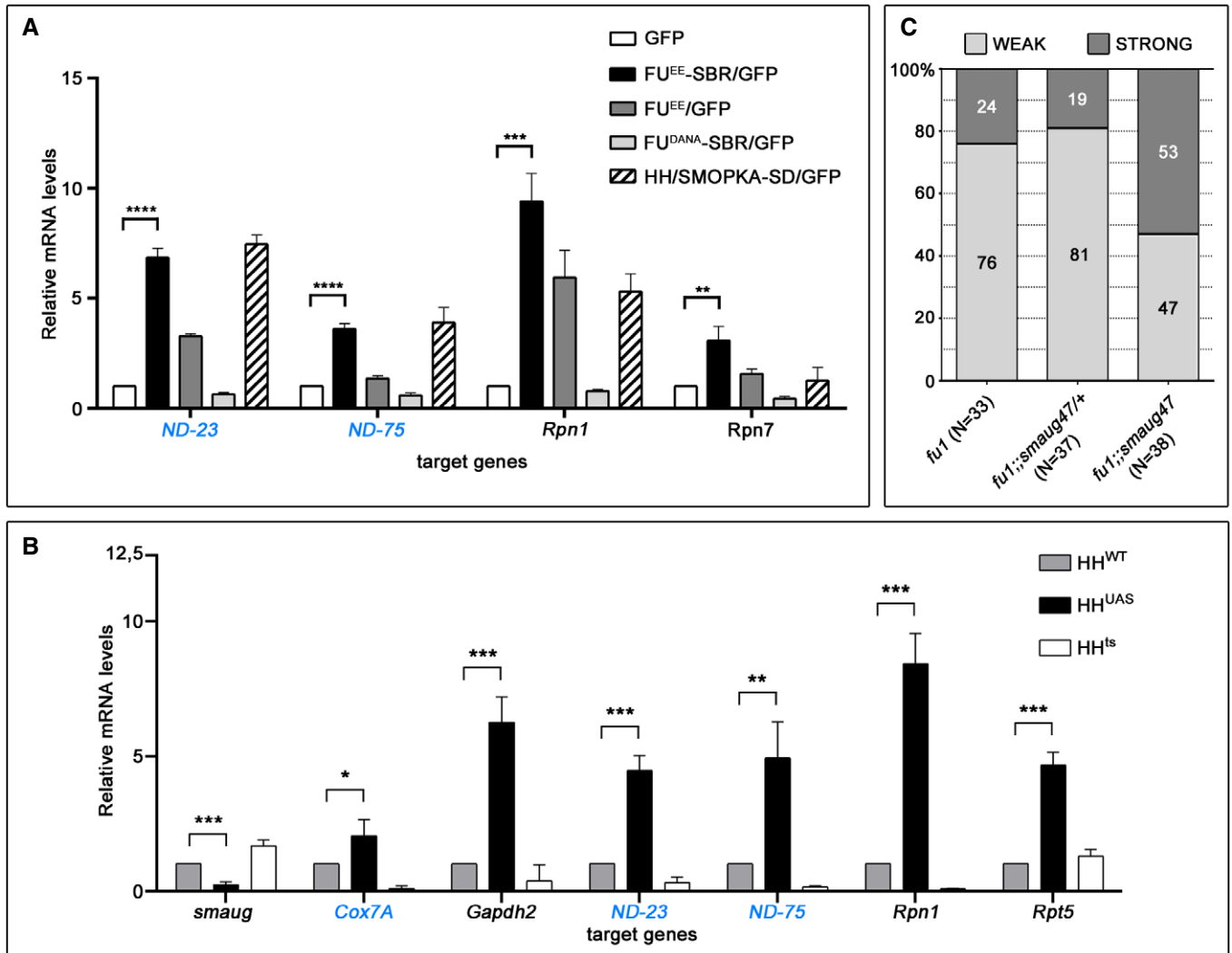
**Figure 5.  HH signaling and Smaug control each other *in vivo*.**

A   Effect of FU^EE^-SBR and HH/SMO on endogeneous Smaug target mRNAs in Cl8 cells. Relative mRNA levels estimated using semi-quantitative RT–PCR for various Smaug's targets in Cl8 cells expressing FU^EE^-SBR (black), FU^EE^ (dark grey), or FU^DANA^-SBR (light grey) were reported with respect to levels of a GFP control. mRNA levels were set to 1 for the GFP control. The list of genes and the sequences of the primers used are shown in Appendix Tables S2 and S3. See also Fig EV5E. Here and in Fig EV5D: RNA encoding mitochondrial proteins are written in blue. *N* = 3 (biological triplicates) and the quantifications were repeated 3 times on each sample. The results are presented as the means ± standard error. The differences between groups were assessed using Student's *t*-tests with Prism V8.2.1 software. A *P* value <0.05 was considered to indicate a statistically significant difference*.

B   Effect of HH on endogeneous targets of Smaug in the wing imaginal disk. Relative levels of Smaug's targets mRNAs in *MS1096; UAS-hh or hh^ts^* and their respective controls (as in Fig EV5X). *N* = 3, with 40 disks for each phenotype.

C   Effect of *smaug* mutation on [fu1] *wing* class distribution. Percent distribution of phenotypic classes (defined in Appendix Fig S4) in *fu^1^* males in presence of zero (*fu^1^*), one (*fu^1^;;smaug^47^/+*), or two copies (*fu^1^;; smaug^47^/smaug^47^*) of the *smaug^47^* allele. The wings were double-blindly classified in "weak" and "strong" according to the LV3-V4 defects (see Fig EV6B). *Chi-square statistical analysis gave a *P* of 0.015 for *fu^1^* and *fu^1^;;smaug^47^/+* distributions and of 0.0024 when comparing *fu^1^;;smaug^47^/+* to *fu^1^;; smaug^47^/smaug^47^*.

levels and the mRNA levels of the reporter, which indicates that this experimental system mainly monitors the effect of Smaug on the decay of its reporter mRNA.

## HH/SMO/FU signaling regulates the RBP Smaug

Modulation of RBP functions can be achieved by controlling their stability, their binding to target mRNAs or to protein co-regulators,

their subcellular localization; and/or ability to form membraneless organelles by liquid–liquid phase separation [3–7,61]. Several of these mechanisms appear to be involved here.

First, HH/SMO/FU signaling controls Smaug's intrinsic repressive action on its target mRNAs, independently of any effect on its levels. This is likely due to a suppression of Smaug promoting the destabilization of mRNAs as HH/SMO/FU leads to a reduction in the levels of its targets mRNA. This effect of HH/SMO/FU requires
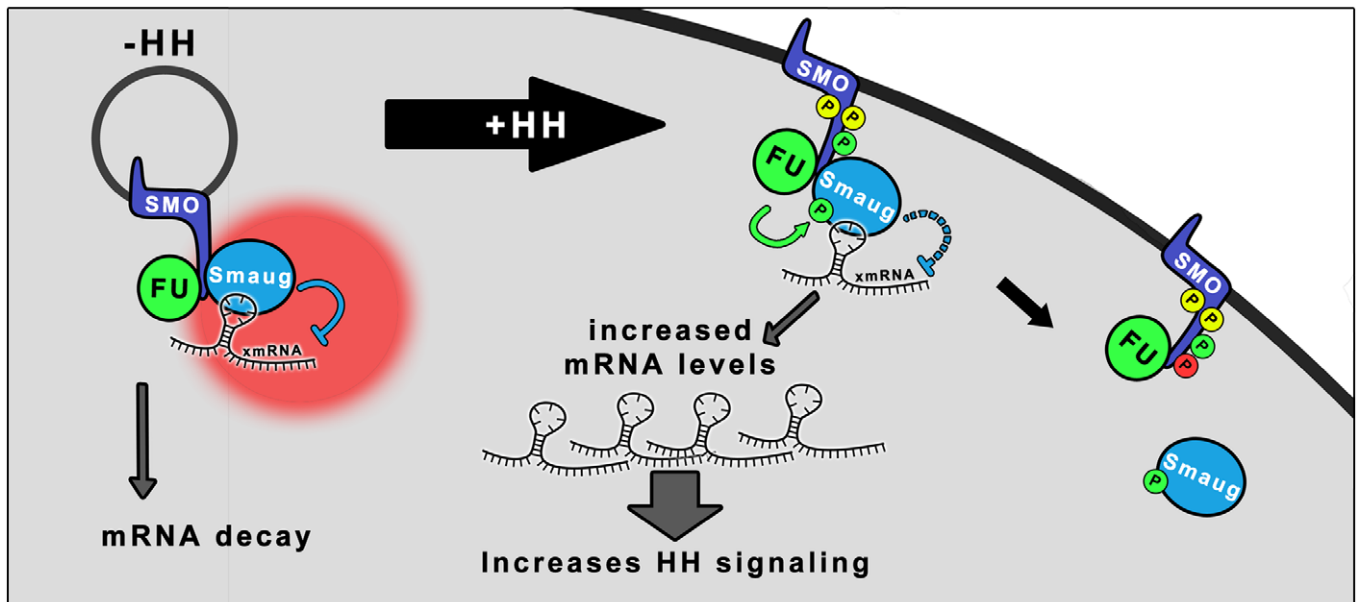
**Figure 6. Model.**

In the absence of HH, Smaug is associated, likely as S-bodies (in red) to inactive SMO present on intracellular vesicles and leads to the repression (blue line) of its target mRNA (s) (called here xmRNA) via the recruitment of proteins (not represented here) that promotes their decay. Upon HH reception, activated and phosphorylated (yellow P circles) SMO accumulates at the plasma membrane where it relocates both the kinase FU and Smaug. This leads to FU activation which in turn phosphorylates (green full circle) SMO and Smaug. This phosphorylation of Smaug would reduce its negative effect (dashed blue line) favoring the release of its target mRNAs—possibly via the dissolution of the S-foci—and leading to their accumulation. Finally, when the highest levels of SMO phosphorylation are reached (red P circle), phosphorylated Smaug is released, leading to attenuation of the effects of HH/SMO/FU on Smaug.

the kinase FU, which promotes Smaug phosphorylation, likely directly (but possibly via another kinase that would remain to be determined). It is also associated with loss of Smaug cytoplasmic bodies that are also triggered by FU. Of note, the regions involved in this phosphorylation contain low-complexity regions (LCR) rich in S/T residues. LCR regions control phase transitions in many RBP [6,62] due to their disordered nature which favors condensate formation via dynamic multivalent interactions [63]. An attractive possibility is that phosphorylation of Smaug in these LCRs could prevent phase transition by introducing negative charges.

Second, HH/SMO/FU also downregulated Smaug levels both in cultured cells and in *in vivo*. This does not require the kinase activity of FU and is associated with a strong reduction in its transcript levels. This reduction is unlikely to reflect a reduced transcription as it was also seen with a *smaug* transcript generated under an exogenous promotor from a plasmid. Given these data, it probably reflects an increase in the decay of Smaug mRNA by a mechanism that remains to be identified. Note that a kinase-independent function of FU has previously been described that probably involves the regulatory C-terminal part, which could act as a scaffolding protein [64,65]. In the present case, it could recruit factors that would promote the destabilization of the *smaug* transcript.

### HH and regulation of mRNA fate

This work strengthens the corpus of emerging connections between HH signaling and the post-transcriptional fate of mRNAs. Most of these studies have focused on the effects of HH signaling on translation in

mammalian cells (reviewed in [66]). Thus, Sonic Hedgehog (Shh) has been shown to have general and specific effects on translation via the activation of key components of translation (for review, see ref. [67]) or via the specific regulation of RBPs. For instance, similarly to its effect on Smaug, Shh controls the phosphorylation of the RBP zipcode-binding protein-1 (ZBP1) during axon guidance [68].

In this context, the present work reveals an additional layer of regulation of HH signaling during wing development that involves the regulation of a RBP by SMO and FU to control mRNA fate, independently of transcription. Indeed, more than half of the mRNAs targeted by Smaug that we tested are also regulated by HH/SMO/FU. Importantly, all the transcripts upregulated by HH/SMO are also upregulated by activated FU when this kinase is artificially tethered to Smaug (and vice versa) but not in the absence of its binding to Smaug. These data strongly indicate that HH/SMO/FU controls Smaug transcripts via their action on Smaug. Strikingly, most of the mRNA targets of Smaug regulated by HH/SMO/FU are not directly linked to signaling processes, but many are involved in proteasome function and metabolism, especially members of the oxidative respiratory chain of the mitochondria. Of note this may be related to the fact that Shh has been shown to affect energy metabolism and mitochondrial function [69,70]. Given that it has been shown that Smaug controls the decay of hundreds, if not thousands of targets, the non-canonical, Smaug-mediated effects that we report here likely affect a wide range of cellular processes.

In conclusion, our data both strengthen the view that Smaug may act as a hub for integration of external information, as has been found for P-bodies and stress granules (for review, see

[71,72]). It also contributes to an emerging paradigm in which signaling and GPCRs can control the fate of mRNAs in the cytoplasm [73].

# Materials and Methods

## Immunoprecipitation

Coimmunoprecipitation in cell lysates: For input (In), 50 μg of protein extract was mixed with loading buffer and frozen in liquid nitrogen before storage overnight at −80°C. For each IP, 1 mg of protein extract was mixed with 2 μg of antibody against the protein tag: mouse anti-HA 12CA5 (Sigma-Aldrich) or rabbit anti-Myc 51c (Euromedex) in 500 μl reaction volume of lysis buffer (RIPA buffer with "Complete EDTA-free antiprotease mix" (Roche)) and Phostop (Roche). IPs were incubated in 1.5-ml tube on a rotating wheel overnight at 4°C. 20 μl Pre-washed Protein A/G Magnetic beads (ThermoScientific) were added for 2 h at 4°C per IP. The beads (IP) were washed three times with cell lysis buffer and re-suspended in 50 μl of 2× Laemmli sample buffer (Bio-Rad) before heating at 95°C for 3 min. For the GFP fusions, coimmunoprecipitation was done using anti-GFP nanobodies cross-linked to NHS resin (1 μg/μl from ChromoTek) and beads were pelleted by centrifugation before loading.

## Western-blotting and immunodetection

Cl8 cells were cultured as previously described in 2% CFS (Hyclone). Transient transfections employed the TransIT-Insect Reagent (Mirus) using a total of 0.5–1 μg of total plasmid DNA for 2–4 μl reactant, respectively. At 48 h post-transfection, cells were washed twice in 1× PBS. After centrifugation, the pellet was lysed in RIPA buffer with the "Complete EDTA free antiprotease mix" (Roche) and the phosphatase inhibitor mix Phostop (Roche), before centrifugation (12,000 rcf) for 10 minutes at 4°C, and then mixed with Laemmli sample buffer (Bio-Rad) and 0.1M DTT. Protein concentrations were estimated with the Bradford Ultra reagent (Expedeon). For direct immunodetection, 60 μg of protein was warmed 5 min at 25°C before loading on a 10% Anderson gel (ratio acrylamide/bis-acrylamide = 77) [74]. Gels were run for 90 min at 150 volts in a Miniprotean (Bio-Rad) apparatus. The subsequent steps were performed as in Ref. [38]. Primary antibodies were as follows: 1:1,000 rat monoclonal anti-HA (Roche), 1:5,000 rabbit anti-GFP (Torrey Pines Biolabs), 1:2,000 rabbit anti-GMAP (Sigma, gift from Laurent Ruel), and 1:1,000 mouse anti-Myc (clone 4A6, Millipore). Secondary antibodies conjugated with HRP were as follows: anti-rat (JacksonImmuno), anti-mouse (Sigma), and anti-rabbit (JacksonImmuno). The enhanced chemiluminescence detection system (ECL Select, Amersham) was used on a LAS-3000 imager (Fujifilm).

## SNAP-Smaug electrophoresis and phosphorylation assay

48 h after transfection, Cl8 cells were lysed in 1% Triton, 50 mM Tris pH 8, 150 mM NaCl, 1 mM DTT with complete EDTA-free antiprotease mix (Roche) before labeling for 30 min at 30°C with 1 μM SNAP-Cell TMR STAR (NEB) alone or together with 1 nM CLIP-Cell TMR STAR (NEB) in 0.66% Triton, 50 mM Tris pH 8, 150 mM NaCl, and 1 mM DTT. Samples were run on a 10% Anderson gel. All gels

of a biological triplicate were run and scanned together on a Typhoon (GE). Images were analyzed and quantified using Imagelab (Bio-Rad) software. Statistical analyses were done using the one-tailed Kruskal–Wallis rank test using GraphPad Prism.

## Cell fluorescent imaging

$5 \times 10^5$ Cl8 cells were plated 24 h (in 24-well plates) before transfection with 250 ng of each plasmid as indicated. In single transfections, pAct.GAL4 was added to ensure a total DNA concentration of 0.5 μg. Cells were analyzed 48hr after transfection. Extracellular SNAP labeling was done by incubation with an extracellular fluorescent substrate SNAP-Surface 488 (NEB) (1.66 μM in Cl8 medium) for 10 min at room temperature before being briefly rinsed 3 times in PBS, fixed for 15 min in 4% PFA, and then washed with PBS three times. Images were taken with a CSU-W1 (Yokogawa-Andor) spinning disk Leica DMI8 microscope with a 63× oil-immersion objective.

## Repression assay

Unless indicated otherwise, the following plasmid concentrations were used for transfection: 300 ng pAct.SNAP-GUS-Stop-5BoxB, 15 ng pAct.λN-SNAP-smaug, 50 ng pAct.GFP-SNAP, 50 ng pAct.smo-GFP (or pAct.smo$^{PKA-SD}$-GFP), and 50 ng pAct.hhN; the total level of DNA was adjusted to 500 ng using pAct.GFP. 48 h after transfection, cells were lysed in 1% Triton, 50 mM Tris pH 8, 150 mM NaCl, 1mM DTT with complete EDTA-free antiprotease mix (Roche) before labeling for 30 min at 37°C with 1.66 nM SNAP-Cell Oregon Green (NEB) in 0.5% Triton, 50 mM Tris pH 8, 150 mM NaCl, and 1 mM DTT. At least three independent biological experiments were performed each time. All gels of a triplicate experiment were run and scanned together. Images were analyzed and quantified using Imagelab (Bio-Rad) software. After quantification, the λN-SNAP-Smaug and SNAP-GUS were normalized to the levels of GFP-SNAP. Statistical analyses were done using the Kruskal–Wallis rank test followed by the Dunn test using GraphPad Prism.

## Relative mRNA quantification

Transfections were done as for the repression assays (see Materials and Methods). Transfected cells were washed in the RNeasy Kit buffer and stored at −80°C until use. Total RNA was isolated from transfected Cl8 cells using RNeasy Kit (NucleoSpin RNA, Macherey-Nagel), and cDNA was synthesized using Superscript III Reverse Transcriptase Kit (Invitrogen). Extraction from wing imaginal disks was performed using xx imaginal disks from third-instar larvae. Quantitative RT–PCR was run in 10 μl reactions in a real-time PCR system (Analytik Jena) using SYBR-Green qPCR Mix (EurobioGreen Lo-ROX, Eurobio). qPCRsoft (3.0) software was used for analyzing cycle threshold (Ct) values. Fold change in RNA levels (expressed as $2^{-\Delta C}$) was normalized to the expression of the Tubulin gene. RT–qPCR was performed in triplicate on each of three independent biological replicates. The sequence of the primers used is given in Appendix Table S3.

## Drosophila strains and genetics

Strains were as follows: w1118, MS1096 (chr. X [75], UAS hh [76], hh$^{ts}$ [77], fu$^1$ [78], and smaug$^{47}$ [13]. Flies were raised at 25°C

unless otherwise indicated. The $w, fu^1/Y;;smaug^{47}/smaug^{47}$ males were obtained by crossing $w, fu^1/Y,$ or FM6;; $smaug^{47}$/TM6 Tb, Sb flies together. The $w, fu^1/Y;;smaug^{47}/+$ males were the progeny from a cross between $fu^1$/FM6;; $smaug^{47}$/TM6 Tb, Sb females with $w^{1118}$ males. The $w, fu^1/+;;$ TM6 Tb, Sb/+ females progeny from this latter cross were mated to $w^{1118}$ males to obtain the $w, fu^1/Y;; +/+$ males. Fly wings were put in 70% ethanol before mounting in Hoyer's medium.

See supplemental materials and methods in Appendix.

**Expanded View** for this article is available online.

## Author contributions

IB, AP, and MS conceived and supervised the experiments. IB, AP, and RAH wrote the manuscript, AP secured funding. GA, MG-A, CA, LB, SM, MS, and FQ performed experiments. LB and MS performed the statistical analysis. IB and MS prepared the figures. GLB, RAH, HDL, and CCS provided reagents, expertise, and feedback.

## Conflict of interest

The authors declare that the research was conducted in the absence of any commercial or financial relationships that could be construed as a potential conflict of interest.

# References

1. Bullock SL (2011) Messengers, motors and mysteries: sorting of eukaryotic mRNAs by cytoskeletal transport. *Biochem Soc Trans* 39: 1161−1165
2. Li Y, Chen G, Wang JY, Zou T, Liu L, Xiao L, Chung HK, Rao JN, Wang JY (2016) Post-transcriptional regulation of Wnt co-receptor LRP6 and RNA-binding protein HuR by miR-29b in intestinal epithelial cells. *Biochem J* 473: 1641−1649
3. Brangwynne CP (2013) Phase transitions and size scaling of membraneless organelles. *J Cell Biol* 203: 875−881
4. Protter DSW, Rao BS, Van Treeck B, Lin Y, Mizoue L, Rosen MK, Parker R (2018) Intrinsically disordered regions can contribute promiscuous interactions to RNP granule assembly. *Cell Rep* 22: 1401−1412
5. Guo L, Shorter J (2015) It's raining liquids: RNA tunes viscoelasticity and dynamics of membraneless organelles. *Mol Cell* 60: 189−192
6. Perez-Pepe M, Fernandez-Alvarez AJ, Boccaccio GL (2018) Life and work of stress granules and processing bodies: new insights into their formation and function. *Biochemistry* 57: 2488−2498
7. Hentze MW, Castello A, Schwarzl T, Preiss T (2018) A brave new world of RNA-binding proteins. *Nat Rev Mol Cell Biol* 19: 327−341
8. Barckmann B, Simonelig M (2013) Control of maternal mRNA stability in germ cells and early embryos. *Biochim Biophys Acta* 1829: 714−724
9. Besse F, Ephrussi A (2008) Translational control of localized mRNAs: restricting protein synthesis in space and time. *Nat Rev Mol Cell Biol* 9: 971−980
10. Laver JD, Ancevicius K, Sollazzo P, Westwood JT, Sidhu SS, Lipshitz HD, Smibert CA (2012) Synthetic antibodies as tools to probe RNA-binding protein function. *Mol BioSyst* 8: 1650−1657
11. Pinder BD, Smibert CA (2013) Smaug: an unexpected journey into the mechanisms of post-transcriptional regulation. *Fly* 7: 142−145
12. Vardy L, Orr-Weaver TL (2007) Regulating translation of maternal messages: multiple repression mechanisms. *Trends Cell Biol* 17: 547−554
13. Chen L, Dumelie JG, Li X, Cheng MH, Yang Z, Laver JD, Siddiqui NU, Westwood JT, Morris Q, Lipshitz HD *et al* (2014) Global regulation of mRNA translation and stability in the early *Drosophila* embryo by the Smaug RNA-binding protein. *Genome Biol* 15: R4
14. Gotze M, Wahle E (2014) Smaug destroys a huge treasure. *Genome Biol* 15: 101
15. Tadros W, Goldman AL, Babak T, Menzies F, Vardy L, Orr-Weaver T, Hughes TR, Westwood JT, Smibert CA, Lipshitz HD (2007) SMAUG is a major regulator of maternal mRNA destabilization in *Drosophila* and its translation is activated by the PAN GU kinase. *Dev Cell* 12: 143−155
16. Jeske M, Moritz B, Anders A, Wahle E (2011) Smaug assembles an ATP-dependent stable complex repressing nanos mRNA translation at multiple levels. *EMBO J* 30: 90−103
17. Rouget C, Papin C, Boureux A, Meunier AC, Franco B, Robine N, Lai EC, Pelisson A, Simonelig M (2010) Maternal mRNA deadenylation and decay by the piRNA pathway in the early *Drosophila* embryo. *Nature* 467: 1128−1132
18. Baez MV, Luchelli L, Maschi D, Habif M, Pascual M, Thomas MG, Boccaccio GL (2011) Smaug1 mRNA-silencing foci respond to NMDA and modulate synapse formation. *J Cell Biol* 195: 1141−1157
19. Chen Z, Holland W, Shelton JM, Ali A, Zhan X, Won S, Tomisato W, Liu C, Li X, Moresco EM *et al* (2014) Mutation of mouse Samd4 causes leanness, myopathy, uncoupled mitochondrial respiration, and dysregulated mTORC1 signaling. *Proc Natl Acad Sci USA* 111: 7367−7372
20. de Haro M, Al-Ramahi I, Jones KR, Holth JK, Timchenko LT, Botas J (2013) Smaug/SAMD4A restores translational activity of CUGBP1 and suppresses CUG-induced myopathy. *PLoS Genet* 9: e1003445
21. Niu N, Xiang JF, Yang Q, Wang L, Wei Z, Chen LL, Yang L, Zou W (2017) RNA-binding protein SAMD4 regulates skeleton development through translational inhibition of Mig6 expression. *Cell Discov* 3: 16050
22. Amadei G, Zander MA, Yang G, Dumelie JG, Vessey JP, Lipshitz HD, Smibert CA, Kaplan DR, Miller FD (2015) A Smaug2-based translational repression complex determines the balance between precursor maintenance versus differentiation during mammalian neurogenesis. *J Neurosci* 35: 15666−15681
23. Aviv T, Lin Z, Lau S, Rendl LM, Sicheri F, Smibert CA (2003) The RNA-binding SAM domain of Smaug defines a new family of post-transcriptional regulators. *Nat Struct Biol* 10: 614−621

24. Green JB, Gardner CD, Wharton RP, Aggarwal AK (2003) RNA recognition via the SAM domain of Smaug. *Mol Cell* 11: 1537–1548

25. Baez MV, Boccaccio GL (2005) Mammalian Smaug is a translational repressor that forms cytoplasmic foci similar to stress granules. *J Biol Chem* 280: 43131–43140

26. Gotze M, Dufourt J, Ihling C, Rammelt C, Pierson S, Sambrani N, Temme C, Sinz A, Simonelig M, Wahle E (2017) Translational repression of the *Drosophila* nanos mRNA involves the RNA helicase Belle and RNA coating by Me31B and Trailer hitch. *RNA* 23: 1552–1568

27. Semotok JL, Cooperstock RL, Pinder BD, Vari HK, Lipshitz HD, Smibert CA (2005) Smaug recruits the CCR4/POP2/NOT deadenylase complex to trigger maternal transcript localization in the early *Drosophila* embryo. *Curr Biol* 15: 284–294

28. Zaessinger S, Busseau I, Simonelig M (2006) Oskar allows nanos mRNA translation in *Drosophila* embryos by preventing its deadenylation by Smaug/CCR4. *Development* 133: 4573–4583

29. Chakravarty AK, Smejkal T, Itakura AK, Garcia DM, Jarosz DF (2019) A non-amyloid prion particle that activates a heritable gene expression program. *Mol Cell* 77: 251–265

30. Lee RT, Zhao Z, Ingham PW (2016) Hedgehog signalling. *Development* 143: 367–372

31. Pak E, Segal RA (2016) Hedgehog signal transduction: key players, oncogenic drivers, and cancer therapy. *Dev Cell* 38: 333–344

32. Claret S, Sanial M, Plessis A (2007) Evidence for a novel feedback loop in the Hedgehog pathway involving Smoothened and Fused. *Curr Biol* 17: 1326–1333

33. Jia J, Tong C, Wang B, Luo L, Jiang J (2004) Hedgehog signalling activity of Smoothened requires phosphorylation by protein kinase A and casein kinase I. *Nature* 432: 1045–1050

34. Formstecher E, Aresta S, Collura V, Hamburger A, Meil A, Trehin A, Reverdy C, Betin V, Maire S, Brun C *et al* (2005) Protein interaction mapping: a *Drosophila* case study. *Genome Res* 15: 376–384

35. Malpel S, Claret S, Sanial M, Brigui A, Piolot T, Daviet L, Martin-Lanneree S, Plessis A (2007) The last 59 amino acids of Smoothened cytoplasmic tail directly bind the protein kinase Fused and negatively regulate the Hedgehog pathway. *Dev Biol* 303: 121–133

36. Chen CH, von Kessler D, Park W, Wang B, Ma Y, Beachy PA (1999) Nuclear trafficking of Cubitus interruptus in the transcriptional regulation of Hedgehog target gene expression. *Cell* 98: 305–316

37. Tang X, Orlicky S, Lin Z, Willems A, Neculai D, Ceccarelli D, Mercurio F, Shilton BH, Sicheri F, Tyers M (2007) Suprafacial orientation of the SCFCdc4 dimer accommodates multiple geometries for substrate ubiquitination. *Cell* 129: 1165–1176

38. Sanial M, Becam I, Hofmann L, Behague J, Arguelles C, Gourhand V, Bruzzone L, Holmgren RA, Plessis A (2017) Dose dependent transduction of Hedgehog relies on phosphorylation-based feedback between the GPCR Smoothened and the kinase Fused. *Development* 144: 1841–1850

39. Chen Y, Jiang J (2013) Decoding the phosphorylation code in Hedgehog signal transduction. *Cell Res* 23: 186–200

40. Denef N, Neubuser D, Perez L, Cohen SM (2000) Hedgehog induces opposite changes in turnover and subcellular localization of patched and smoothened. *Cell* 102: 521–531

41. Nakano Y, Nystedt S, Shivdasani AA, Strutt H, Thomas C, Ingham PW (2004) Functional domains and sub-cellular distribution of the Hedgehog transducing protein Smoothened in *Drosophila*. *Mech Dev* 121: 507–518

42. Behm-Ansmant I, Rehwinkel J, Doerks T, Stark A, Bork P, Izaurralde E (2006) mRNA degradation by miRNAs and GW182 requires both CCR4:NOT deadenylase and DCP1:DCP2 decapping complexes. *Genes Dev* 20: 1885–1898

43. Pillai RS, Artus CG, Filipowicz W (2004) Tethering of human Ago proteins to mRNA mimics the miRNA-mediated repression of protein synthesis. *RNA* 10: 1518–1525

44. Rehwinkel J, Behm-Ansmant I, Gatfield D, Izaurralde E (2005) A crucial role for GW182 and the DCP1:DCP2 decapping complex in miRNA-mediated gene silencing. *RNA* 11: 1640–1647

45. Tirat A, Freuler F, Stettler T, Mayr LM, Leder L (2006) Evaluation of two novel tag-based labelling technologies for site-specific modification of proteins. *Int J Biol Macromol* 39: 66–76

46. Battle LJ, Chambers TC (2017) Small peptide substrates and high resolution peptide gels for the analysis of site-specific protein phosphorylation and dephosphorylation. *J Biol Methods* 4: e76

47. Su Y, Ospina JK, Zhang J, Michelson AP, Schoen AM, Zhu AJ (2011) Sequential phosphorylation of smoothened transduces graded hedgehog signaling. *Sci Signal* 4: ra43

48. Dussillol-Godar F, Brissard-Zahraoui J, Limbourg-Bouchon B, Boucher D, Fouix S, Lamour-Isnard C, Plessis A, Busson D (2006) Modulation of the Suppressor of fused protein regulates the Hedgehog signaling pathway in *Drosophila* embryo and imaginal discs. *Dev Biol* 291: 53–66

49. Ruel L, Gallet A, Raisin S, Truchi A, Staccini-Lavenant L, Cervantes A, Therond PP (2007) Phosphorylation of the atypical kinesin Costal2 by the kinase Fused induces the partial disassembly of the Smoothened-Fused-Costal2-Cubitus interruptus complex in Hedgehog signalling. *Development* 134: 3677–3689

50. Fukumoto T, Watanabe-Fukunaga R, Fujisawa K, Nagata S, Fukunaga R (2001) The fused protein kinase regulates Hedgehog-stimulated transcriptional activation in *Drosophila* Schneider 2 cells. *J Biol Chem* 276: 38441–38448

51. Zhou Q, Kalderon D (2011) Hedgehog activates fused through phosphorylation to elicit a full spectrum of pathway responses. *Dev Cell* 20: 802–814

52. Shi Q, Li S, Jia J, Jiang J (2011) The Hedgehog-induced Smoothened conformational switch assembles a signaling complex that activates Fused by promoting its dimerization and phosphorylation. *Development* 138: 4219–4231

53. Han Y, Wang B, Cho YS, Zhu J, Wu J, Chen Y, Jiang J (2019) Phosphorylation of Ci/Gli by fused family kinases promotes hedgehog signaling. *Dev Cell* 50: 610–626.e614

54. Chartier A, Klein P, Pierson S, Barbezier N, Gidaro T, Casas F, Carberry S, Dowling P, Maynadier L, Bellec M *et al* (2015) Mitochondrial dysfunction reveals the role of mRNA poly(A) tail regulation in oculopharyngeal muscular dystrophy pathogenesis. *PLoS Genet* 11: e1005092

55. Dahanukar A, Walker JA, Wharton RP (1999) Smaug, a novel RNA-binding protein that operates a translational switch in *Drosophila*. *Mol Cell* 4: 209–218

56. Therond P, Alves G, Limbourg-Bouchon B, Tricoire H, Guillemet E, Brissard-Zahraoui J, Lamour-Isnard C, Busson D (1996) Functional domains of fused, a serine-threonine kinase required for signaling in *Drosophila*. *Genetics* 142: 1181–1198

57. Pascual ML, Luchelli L, Habif M, Boccaccio GL (2012) Synaptic activity regulated mRNA-silencing foci for the fine tuning of local protein synthesis at the synapse. *Commun Integr Biol* 5: 388–392

58. Luchelli L, Thomas MG, Boccaccio GL (2015) Synaptic control of mRNA translation by reversible assembly of XRN1 bodies. *J Cell Sci* 128: 1542–1554

59. Fernandez-Alvarez AJ, Pascual ML, Boccaccio GL, Thomas MG (2016) Smaug variants in neural and non-neuronal cells. *Commun Integr Biol* 9: e1139252

60. Nelson MR, Leidal AM, Smibert CA (2004) *Drosophila* Cup is an eIF4E-binding protein that functions in Smaug-mediated translational repression. *EMBO J* 23: 150−159

61. Lovci MT, Bengtson MH, Massirer KB (2016) Post-translational modifications and RNA-binding proteins. *Adv Exp Med Biol* 907: 297−317

62. Wang JT, Smith J, Chen BC, Schmidt H, Rasoloson D, Paix A, Lambrus BG, Calidas D, Betzig E, Seydoux G (2014) Regulation of RNA granule dynamics by phosphorylation of serine-rich, intrinsically disordered proteins in *C. elegans*. *Elife* 3: e04591

63. Calabretta S, Richard S (2015) Emerging roles of disordered sequences in RNA-binding proteins. *Trends Biochem Sci* 40: 662−672

64. Alves G, Limbourg-Bouchon B, Tricoire H, Brissard-Zahraoui J, Lamour-Isnard C, Busson D (1998) Modulation of Hedgehog target gene expression by the Fused serine-threonine kinase in wing imaginal discs. *Mech Dev* 78: 17−31

65. Robbins DJ, Nybakken KE, Kobayashi R, Sisson JC, Bishop JM, Therond PP (1997) Hedgehog elicits signal transduction by means of a large complex containing the kinesin-related protein costal2. *Cell* 90: 225−234

66. D'Amico D, Canettieri G (2016) Translating hedgehog in cancer: controlling protein synthesis. *Trends Mol Med* 22: 851−862

67. Charron F (2017) Linking Hedgehog, Translation, and mTORC1 in Medulloblastoma. *Dev Cell* 43: 655−656

68. Lepelletier L, Langlois SD, Kent CB, Welshhans K, Morin S, Bassell GJ, Yam PT, Charron F (2017) Sonic hedgehog guides axons via zipcode binding protein 1-mediated local translation. *J Neurosci* 37: 1685−1695

69. Shigunov P, Balvedi LT, Santos MDM, Herai RH, de Aguiar AM, Dallagiovanna B (2018) Crosstalk between Hedgehog pathway and energy pathways in human adipose-derived stem cells: a deep sequencing analysis of polysome-associated RNA. *Sci Rep* 8: 8411

70. Yao PJ, Manor U, Petralia RS, Brose RD, Wu RT, Ott C, Wang YX, Charnoff A, Lippincott-Schwartz J, Mattson MP (2017) Sonic hedgehog pathway activation increases mitochondrial abundance and activity in hippocampal neurons. *Mol Biol Cell* 28: 387−395

71. Buchan JR (2014) mRNP granules. Assembly, function, and connections with disease. *RNA Biol* 11: 1019−1030

72. Kedersha N, Ivanov P, Anderson P (2013) Stress granules and cell signaling: more than just a passing phase? *Trends Biochem Sci* 38: 494−506

73. Trefier A, Pellissier LP, Musnier A, Reiter E, Guillou F, Crepieux P (2018) G protein-coupled receptors as regulators of localized translation: the forgotten pathway? *Front Endocrinol (Lausanne)* 9: 17

74. Anderson CW, Baum PR, Gesteland RF (1973) Processing of adenovirus 2-induced proteins. *J Virol* 12: 241−252

75. Capdevila J, Pariente F, Sampedro J, Alonso JL, Guerrero I (1994) Subcellular localization of the segment polarity protein patched suggests an interaction with the wingless reception complex in *Drosophila* embryos. *Development* 120: 987−998

76. Ingham PW, Fietz MJ (1995) Quantitative effects of hedgehog and decapentaplegic activity on the patterning of the *Drosophila* wing. *Curr Biol* 5: 432−440

77. Ma C, Zhou Y, Beachy PA, Moses K (1993) The segment polarity gene hedgehog is required for progression of the morphogenetic furrow in the developing *Drosophila* eye. *Cell* 75: 927−938

78. Busson D, Limbourg-Bouchon B, Mariol MC, Préat T, Lamour Isnard C (1988) Genetic analysis of viable and lethal fused mutants of *Drosophila* melanogaster. *Roux Arch Dev Biol* 197: 221−230

79. Maier D, Cheng S, Faubert D, Hipfner DR (2014) A broadly conserved g-protein-coupled receptor kinase phosphorylation mechanism controls *Drosophila* smoothened activity. *PLoS Genet* 10: e1004399

80. Zhang C, Williams EH, Guo Y, Lum L, Beachy PA (2004) Extensive phosphorylation of Smoothened in Hedgehog pathway activation. *Proc Natl Acad Sci USA* 101: 17900−17907